Hindawi
Advances in Civil Engineering
Volume 2023, Article ID 4571162, 14 pages
https://doi.org/10.1155/2023/4571162

Research Article

Research on the Performance of Calcium Carbide Slag–Fly Ash Stabilized Soil

Yanxia Cai,[1,2,3] Zhishu Zang,[4] Xiaolin Zuo,[5] Fengtao Liu,[5] Lengxue Li,[5] Kaiji Lu,[1,2,3] and Qianlong Huang[1,2,3]

[1]*Beijing Zhonglu Gaoke Highway Technology Co. Ltd., Beijing 100088, China*
[2]*Research and Development Center of Transport Industry of New Materials, Technologies Application for Highway Construction and Maintenance, Beijing 100088, China*
[3]*Research Institute of Highway Ministry of Transport, Beijing 100088, China*
[4]*China Highway Engineering Consulting Corporation, Beijing 100097, China*
[5]*Handan Zhongjian Hengzhi Engineering Project Management Co. Ltd., Handan 056000, China*

Correspondence should be addressed to Zhishu Zang; zangzhishu@checc.com.cn and Qianlong Huang; hql806438934@163.com

Received 23 December 2022; Revised 31 July 2023; Accepted 8 August 2023; Published 24 August 2023

Academic Editor: Xing Wang

To address the scarcity of lime resources, this study explores the potential of using industrial solid waste, including fly ash (FA) and carbide slag, as replacements for lime or cement in soil stabilization for roadbed construction. The optimal mixing ratio of FA and calcium carbide slag (CCS) was determined using compaction and unconfined compressive tests. The study also examines the relationship between the optimum moisture content and the maximum dry density of the FA and CCS binder, as well as the strength variation trend. The study investigated the optimal mixing ratio of FA–CCS-stabilized soil, and the strength variation trend of FA and carbide slag-stabilized soil under different age and mixing ratios, using tests such as the unconfined compressive energy test, splitting strength test, compressive modulus of resilience test, and California bearing ratio test. Results indicate that the optimal mixing ratio of FA and CCS binder is 1 : 4, the advocated mixing ratio of CCS-stabilized soil is 8 : 92, and the excellent mixing ratio of CCS–FA-stabilized soil is 8 : 32 : 60.

1. Introduction

Based on statistical data [1], the total length of toll roads in China reached 5,354,800 km by the end of 2022, with category II and above highways accounting for 743,600 km (including 177,300 km of expressways), representing 13.9% of the total toll road mileage. Currently, the construction of expressways is rapidly increasing, leading to a higher demand for road construction materials [2]. However, limestone, a commonly used material in road construction, is a nonrenewable resource with limited availability [3]. Therefore, finding a new material to replace lime or cement is urgently needed in the road construction industry.

Fly ash (FA) is a fine solid particle in the flue gas ash produced by fuel combustion. It is an industrial byproduct with high strength and strong plate properties. It mainly contains silicon dioxide (SiO_2), aluminum oxide (Al_2O_3), and iron oxide (Fe_2O_3). It has been widely used to make various light building materials [4]. Calcium carbide slag (CCS) is an industrial waste residue after acetylene gas is obtained from calcium carbide hydrolysis. The main component is calcium hydroxide [$Ca(OH)_2$] [5]. Using CCS can replace limestone to make cement, produce quicklime as calcium carbide raw material, produce chemical products, produce building materials and be used for environmental treatment [6, 7].

In order to verify the feasibility of using FA and CCS as stabilizing materials to replace lime or cement, many scholars have conducted relevant experimental studies on FA and CCS-stabilized soil [8–10]. Nergis et al. [11] analyzed the effect of aggregates on local FA-based geopolymers from a structural and mechanical perspective. The study found that aggregates significantly affect the density, compression strength, and flexural strength of samples at all ages. Sinan

et al. [12] reviewed the effect of FA application on soil characteristics. In general, it is widely acknowledged that FA improves soil stability, water-holding capacity, and bulk density and raises the low pH in soil. However, it has been found that this beneficial effect is observed only at moderate levels, whereas higher levels can have a significant depressing effect. Mashifana et al. [13] investigated the effect of the geotechnical properties and microstructure of expansive soil stabilized with phosphogypsum-lime-FA-basic oxygen furnace slag paste. The soil microstructure was improved due to the formation of hydration products. The stabilized expansive soil met the specification for road subgrades and subbases. Nath et al. [14] studied the effects of FA on the consistency, compactness, acidity, and strength of organic soil. It was observed that the addition of FA significantly reduces the plasticity index of organic soil, while the liquid and plastic limits increase. Moreover, the dry density of FA–soil mixture increases significantly, while the water requirement decreases due to the addition of FA. Increased dry density affects higher strength. Qin et al. [15] studied the performance comparison of stabilized soil with CCS and lime under the same output through laboratory tests. The test results show that when the content of CCS and lime is the same, the performance of stabilized soil with CCS is better than that of stabilized soil with lime. To optimize the composition and proportion of CCS-stabilized soil, Li et al. [16] analyzed the change in compressive strength of stabilized soil under different compaction conditions and investigated the influence law of soil plasticity index, clay content, and colloidal activity index on the optimal CCS dosage. The results showed that the unconfined compressive strength of CCS-stabilized soil could meet the requirements of the lime-stabilized material specification. Leong et al. [17] analyzed the significant variables affecting the compressive strength of FA-soil polymer using a variable analysis approach based on neural networks and genetic planning. The evaluation results identified the percentage of FA, water, and soil as important input variables for output. The percentage of hydroxides, the ratio of silicates to hydroxides, and the ratio of alkali activator to ashes were considered less important input variables. The positive or negative correlation between these input variables and the output has a significant impact on the strength development of FA–soil polymer and can have a positive or negative influence on compressive strength. Si/Al molar ratio can serve as a dimensionless index of raw materials for alkali-activated materials (AAM) quality control, according to potential solution. In the article, a comprehensive review was conducted from the perspective of Si/Al molar ratio, and its correlation with various AAM properties was summarized. The feasibility of producing AAM using the molar ratio while maintaining stable performance was verified. Based on this, a three-step strategy was proposed, which can more effectively transform a wider range of waste with high variability into normalized AP and provide guidance for waste valorization and AAM quality control [18].

Numerous scholars have studied the performance of CCS in improving different soil properties. Wei et al. [19] conducted indoor testing to investigate the efficacy of using CCS for soil improvement in saline soil. Their results indicate a reduction in the plasticity index and an increase in optimal water content and bearing capacity of the improved saline soil. Xiao [20] conducted a systematic study on the behavior of CCS-improved expansive soil. The results from their matrix suction testing show that the cohesion of the CCS-improved soil increases with curing age, while overall cohesion decreases with the increase of cycle times. Latifi et al. [21] conducted an experimental study on the mechanical properties of expansive soil and kaolin stabilized with CCS. The results showed that with the increase in the amount of CCS, the compressive strength of the improved soil increased by about 4.7–6.8 times compared with that of the undisturbed soil. The improvement effect on kaolin was more significant, and the compressive strength increased by about 3.8–5.8 times.

In summary, many scholars have conducted extensive research on CCS-stabilized soil and FA-stabilized soil. However, the strength of these types of soils is influenced by numerous factors, and there is a limited amount of research on the strength formation mechanism and mechanical properties of CCS–FA-stabilized soil. Further research is needed to investigate the strength formation mechanism and mechanical properties of CCS–FA-stabilized soil at different ages.

This paper compares and studies the influence of different mixing proportions of CCS and FA on the mechanical properties of CCS–FA-stabilized soil at different ages through indoor compaction tests and unconfined compressive strength tests. The results demonstrate the feasibility of using CCS–FA-stabilized soil for roadbed treatment and mine repair and provide valuable insights into the application of CCS and FA in subgrade engineering.

2. Materials

2.1. Basic Physical and Chemical Properties of CCS. CCS refers to the industrial waste discharged by a gas company in Handan, Hebei, China. The basic physical properties of CCS are presented in Table 1, and the chemical composition is shown in Table 2.

It can be seen from Table 2 that the main component of CCS is CaO, followed by SiO_2 and Al_2O_3, the content of MgO in CCS is only 0.34%, so CCS belongs to calcareous slaked lime.

The test results of calcium and magnesium content and water content of CCS (see Figure 1).

As shown in Figure 1, the initial calcium and magnesium content of simplified industrial calcareous slag (CCS) was 76%, and the water content was 47%. However, after being stored under room temperature and natural ventilation conditions for about 45 days, the calcium and magnesium content decreased to 62%, and the water content was 11%, which met the requirements for the use of grade II hydrated lime. After 90 days, the calcium and magnesium content stabilized at around 56%, and the water content was approximately 6%. The decrease in calcium and magnesium content was mainly due to the reaction between calcium and magnesium hydroxides and CO_2 in the air, generating carbonate oxides.

Table 1: Basic physical properties of CCS.

Type	Morphology	Color	Moisture content (%)	Bulk density (g/cm^3)	Smell	Loss on ignition (%)
Natural CCS	Condense into clumps	Dark gray	35%–40%	0.89	Pungent odor	29.1
Dry CCS	Powdered	white	0	—		

Table 2: Chemical composition of CCS.

Ingredients	CaO	SiO_2	Al_2O_3	ZnO	Fe_2O_3	MgO	SO_3	TiO_2	Other
Content (%)	91.08	4.26	2.36	0.79	0.40	0.34	0.34	0.08	0.35

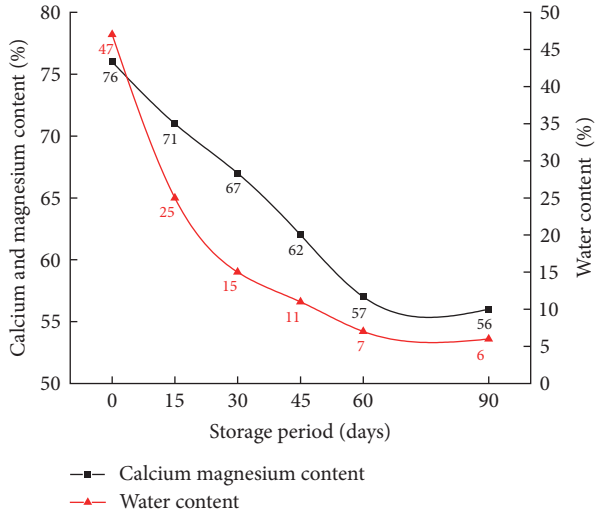

Figure 1: Changes in calcium and magnesium content and water content of CCS.

The linear decrease in calcium and magnesium content from 0 to 60 days indicates that the internal reaction process is uniform.

In summary, based on the test results, if CCS is utilized as a stabilizing material for expansive soil, its storage period should not exceed 45 days. If the storage period exceeds 45 days, it fails to conform to the usage specifications for the calcium and magnesium content of hydrated lime specified in the guidelines.

2.2. Basic Physical and Chemical Properties of FA. The physical and chemical properties of FA were analyzed and investigated in accordance with the test code for inorganic binder stabilized materials in Highway Engineering (JTG E51-2009). The test results are presented in Table 3, and the chemical composition is shown in Table 4.

As shown in Table 3, the fineness of the FA is 37.3%, indicating that it belongs to grade III FA. This light material possesses a large specific surface area, which is favorable for the cementation reaction with stabilizing materials. The liquid plastic limit is high, but the plasticity index is low.

Based on the data presented in Table 4, the primary chemical constituents of the FA are SiO_2 and Al_2O_3, indicating that it is a silicon aluminum FA. Indoor tests indicate that the calcium ions in the FA exist in the form of $CaCO_3$.

2.3. Basic Physical Properties of Soil Samples. The basic physical properties of soil samples are examined and analyzed in accordance with the specifications for highway soil tests (JTG E40-2007), and the results are presented in Table 5.

As shown in Table 5, the soil sample is well-graded and classified as a nonexpansive clay with a low liquid limit, and all indicators meet the technical requirements specified in the standard.

3. Methodology

3.1. Test Scheme. The objective of selecting CCS and FA-stabilized soil is to optimize resource utilization, reduce the excessive use of lime cement and other materials, and recognize the high-value potential of these resources. A range of FA and CCS mix ratios were evaluated, including 10 : 90, 20 : 80, 25 : 75, 33 : 67, 50 : 50, 67 : 33, 75 : 25, 80 : 20, and 90 : 10. The optimum moisture content and maximum dry density were determined through compaction tests, and the best mix ratio was established based on the unconfined compressive strength at 7 and 28 days. The mechanical properties of the stabilized soil were then studied using the chosen FA and CCS ratio. Various CCS contents, including 4%, 6%, 8%, 10%, and 12%, were tested. Indoor tests were conducted on both CCS-stabilized soil and CCS–FA-stabilized soil at the optimal mix ratio.

3.2. Compaction Test Method. In the compaction test, the multifunctional automatic electric compaction instrument (refer to Figure 2) was utilized. The test materials were passed through a 4.75 mm square hole sieve and sampled using the quartering method. Subsequently, soil and CCS were mixed with water in a calculated proportion according to the predetermined water content and then sealed in a bag for over 12 hr. The compaction was completed using a compaction cylinder with an inner diameter, height, volume, and weight of 10, 12.7, 997 cm^3, and 4.5 kg, respectively. The punching surface diameter was 5 cm with an average punching work unit of 2.687 J. The compaction process was conducted in five layers, with each layer being brushed between hammering and being hammered 27 times. The sample was finally demolded using an electric demolding instrument (refer to Figure 3). The compaction of FA and CCS was checked, and the test results are presented in Figure 4.

As shown in Figure 4, decreasing the proportion of FA (and increasing the proportion of CCS) leads to a gradual

Table 3: Basic physical properties of FA.

Fineness (%)	Density (g/cm^3)	Specific gravity	Specific surface area (cm^2/g)	Burning loss	Liquid limits	Plastic limit	Plasticity index
37.3	2.12	2.2	5,256	17.6	32.8	28.4	4.4

Table 4: Chemical composition of FA.

Chemical composition	SiO_2	Al_2O_3	Fe_2O_3	CaO	K_2O	TiO_2	MgO	SO_3	Na_2O	Other
Content (%)	52.69	34.82	3.79	2.61	1.53	1.13	1.04	0.80	0.65	0.94

Table 5: Basic physical properties of soil samples.

Water content (%)	Specific gravity	Liquid limits (%)	Plastic limit (%)	Plasticity index	Optimum moisture content (%)	Maximum dry density (g/cm^3)
14.6	2.56	32.6	21.0	11.5	13.2	1.818

Figure 2: Multifunctional automatic electric compactor.

Figure 3: Electric demolding instrument.

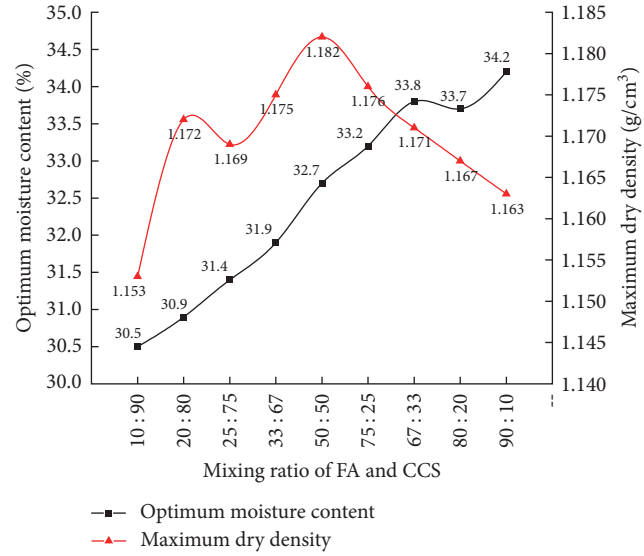

Figure 4: The changing trend of FA and CCS compaction test.

increase in the optimal water content of the CCS–FA-stabilized soil, while the maximum dry density first increases and then decreases.

The ultimate water content material of CCS–FA gradually increases because the important elements of CCS are CaO, and the principal aspects of FA are SiO_2 and Al_2O_3. CCS exhibits properties similar to hydrated lime, as it can easily ionize and hydrolyze in water, generating Ca^{2+} and OH^- ions. CCS and FA are also prone to pozzolanic reactions, which can react with silicon, aluminum, and other components, generating a large number of C–S–H and C–A–H crystals. These reactions require a significant amount of water, and therefore, the optimal water content of the CCS–FA binder gradually increases with an increase in FA content.

The maximum dry density of the CCS–FA-stabilized soil first increases and then decreases, primarily due to the small surface area of FA particles, while the pores between CCS

Figure 5: Universal material testing machine.

Figure 6: The pavement strength testing machine.

particles are relatively large. When the proportion of FA is less than 50%, the pores between its internal particles are compacted under the action of compaction work, resulting in a gradual increase in dry density. However, when the proportion of FA exceeds 50%, the content of CCS decreases significantly, often due to the skeleton effect between FA particles, which is gradually compacted under the action of compaction work, leading to a decrease in dry density [22].

3.3. Unconfined Compressive Strength of Binder. The unconfined compressive strength was primarily determined using a universal material testing machine, an electric stripper, and a pavement strength testing machine, as illustrated in Figures 5 and 6. Cylindrical specimens with a diameter and height of 50 mm were utilized. Initially, the mixed materials, with varying proportions, were statically pressed using the universal material testing machines, based on the optimum water content and maximum dry density obtained from the compaction test. Subsequently, the mixed materials were sealed using plastic bags via the electric stripper. After standard curing to the specified age, the pavement strength tester was employed to conduct the unconfined compressive strength test, with the results shown in Figure 7 for CCS–FA.

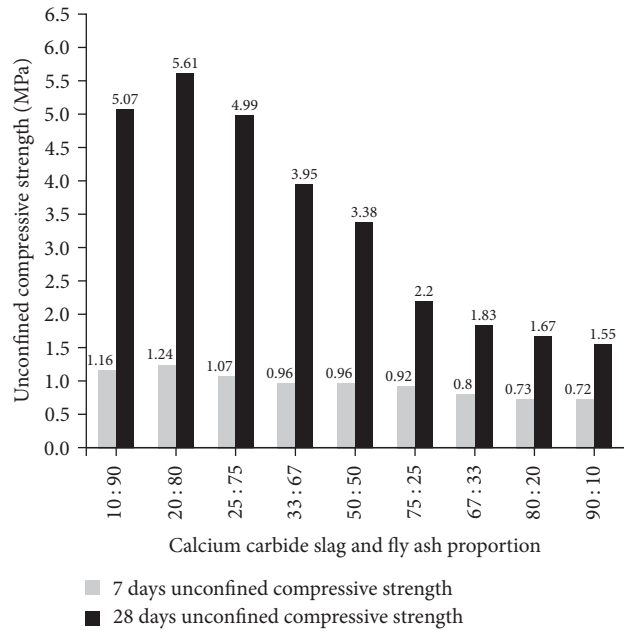

Figure 7: Unconfined compressive strength changes of calcium carbide slag and fly ash.

Figure 7 illustrates that the proportion of CCS and FA initially increases and subsequently decreases. The peak value of unconfined compressive strength is attained when the proportion of CCS and FA is 20 : 80 or 1 : 4, with maximum values of 1.24 and 5.61 MPa, respectively. The 28 day strength growth rate varies between 2.15% and 4.66% for different proportions of CCS and FA, indicating a rapid increase in early strength for the CCS and FA binder. Therefore, it can be concluded that the optimal mixing ratio of CCS and FA is 1 : 4 [8].

3.4. Strength Formation Mechanism of Improved Soil

3.4.1. Formation Mechanism of CCS Stabilized Soil Strength. The formation mechanism of CCS strength is very similar to that of lime-stabilized soil, which can be summarized into four stages [23]:

(*1*) *Ion Exchange Reaction*. The clay surface typically carries a negative charge. Upon adding calcium oxide in CCS to water for decomposition, ion exchange reactions occur, leading to the formation of a stable structure and an increase in the overall strength. This is one of the primary reasons for the early strength development of the CCS-FA-stabilized soil.

(*2*) *Volcanic Ash Reaction*. The reaction of $Ca(OH)_2$ in the soil with silicon and aluminum in CCS leads to the formation of C–S–H and C–A–H. This reaction not only enhances the cohesion between the stabilized materials but also sustains their strength growth over time. The chemical reaction equation is as follows:

$$xCa(OH)_2 + SiO_2 + nH_2O \rightarrow xCa \cdot SiO_2(n+1)H_2O. \quad (1)$$

$$xCa(OH)_2 + Al_2O_3 + nH_2O \rightarrow xCa \cdot Al_2O_3(n+1)H_2O. \quad (2)$$

(3) *Carbonation*. Carbonation is mainly due to the formation of $CaCO_3$ from Ca $(OH)_2$ in CCS by H_2O and CO_2 in the air. The reaction formula is as follows:

$$CaO + H_2O = Ca(OH)_2. \quad (3)$$

$$Ca(OH)_2 + CO_2 = CaCO_3 + H_2O. \quad (4)$$

The experiment demonstrates that the carbonation reaction requires the presence of water to occur. When the environment contains only dry CO_2 and $Ca(OH)_2$ powder, the reaction is nearly halted. Hence, the reaction formula expressed as Formula (5) is more practical.

$$Ca(OH)_2 + nH_2O + CO_2 \rightarrow CaCO_3 + (n+1)H_2O. \quad (5)$$

(4) *Crystallization*. The carbonation reaction impedes the penetration of CO_2 into the structure, thereby impeding further reactions. In the stabilized soil, $Ca(OH)_2$ crystals are produced spontaneously, which further augments the strength of the improved soil. The reaction can be expressed with the following formula:

$$Ca(OH)_2 + nH_2O \rightarrow Ca(OH)_2 \cdot nH_2O. \quad (6)$$

Based on the reactions in the four stages described above, the strength of the CCS–FA-stabilized soil improves gradually. The early strength is primarily due to the volcanic ash reaction, while the hydrolysis of CCS is a prerequisite for all reactions. The stabilized soil forms its initial strength through ion exchange and condensation, and the strength of the stabilized soil is further improved through crystallization and carbonation.

3.4.2. CCS–FA-Stabilized Soil Strength Formation Mechanism. The strength mechanism of the stabilized soil using CCS and FA is essentially the same and primarily involves the following processes [24]:

(1) Formation of a silicon–aluminum thin layer on particle surfaces. After mixing with water, CCS and FA become saturated with $Ca(OH)_2$ in the alkaline liquid phase. Water combines with FA to ionize SiO_4^{4-} and H^+, leading to a negatively charged FA surface. Due to gravitational effects, Ca^{2+} is adsorbed onto the FA surface, causing K^+ and Na^+ to dissolve and resulting in the formation of additional silicon–aluminum thin layers on the FA surface.

(2) Presence of a precipitated blanket. Following the formation of the thin layer, SiO_4^{4-} and AlO_2^{2-} gradually precipitate from the surface layer and combine with the surrounding Ca^{2+} to form a thick layer of precipitation.

(3) The sediment coating is broken when the concentration of any ion in the liquid phase of the particles and the cladding layer is greater than the concentration of the outer layer, it will expand and gradually break, and the interaction between ions will form a new cladding layer, which is a continuous cycle process.

(4) Formation of hydrated calcium silicate and calcium aluminate with the increase of ion concentration in the coating, Ca^{2+} is adsorbed on the surface of the coating, forming C–A–H and C–S–H precipitates.

4. Result Analysis

4.1. Compaction Test. Figure 8 shows the optimum moisture content and maximum dry density of CCS-stabilized soil and CCS–FA-stabilized soil. In the reference group, the optimum moisture content of 4% cement-stabilized soil was 11.2%, and the maximum dry density was 1.842 g/cm^3.

Based on the results of the compaction test presented in Figure 8, it can be observed that the plain soil has an optimum moisture content of 13.2% and a maximum dry density of 1.878 g/cm^3. On the other hand, the maximum dry density of CCS-stabilized soil ranges from 1.868 to 1.806 g/cm^3, while for CCS–FA-stabilized soil, it ranges from 1.642 to 1.312 g/cm^3. Regarding the optimal water content, it is noteworthy that 4% cement soil has an optimal water content of 11.2%. Meanwhile, for CCS-stabilized soil, the optimal water content ranges from 11.6% to 14.6%, and for CCS–FA-stabilized soil, it ranges from 18.8% to 23.6%. One possible reason for this is that, compared to cement-stabilized soil, CCS–FA-stabilized soil produces some flocculent cementation products that result in a certain volume expansion, thereby reducing soil compactness and density. Conversely, the optimum water content tends to continuously increase, which is mainly related to the strength mechanism of CCS–FA-stabilized soil. As the ion-exchange and pozzolanic reactions progress continuously, the contact between soil particles and binder is enhanced, and recombination between particles requires the auxiliary action of more free water. This causes the water required for improved soil to continuously increase [25, 26]. The water content of CCS–FA-stabilized soil is higher than that of CCS-stabilized soil, indicating that the addition of FA intensifies the ion-exchange and pozzolanic reactions of stabilized soil [27, 28].

4.2. Unconfined Compressive Strength Test. The unconfined compressive strength tests were conducted following the method T0805-1994 outlined in JTG E51-2009, and the results are presented in Figure 9. Figure 10 shows a comparison of the compressive strengths of CS, 4% cement soil, and FCS. In the reference group, the 7, 28, 60, and 90 days unconfined compressive strengths of 4% cement-stabilized soil were 1.32, 1.54, 1.68, and 2.52 MPa, respectively.

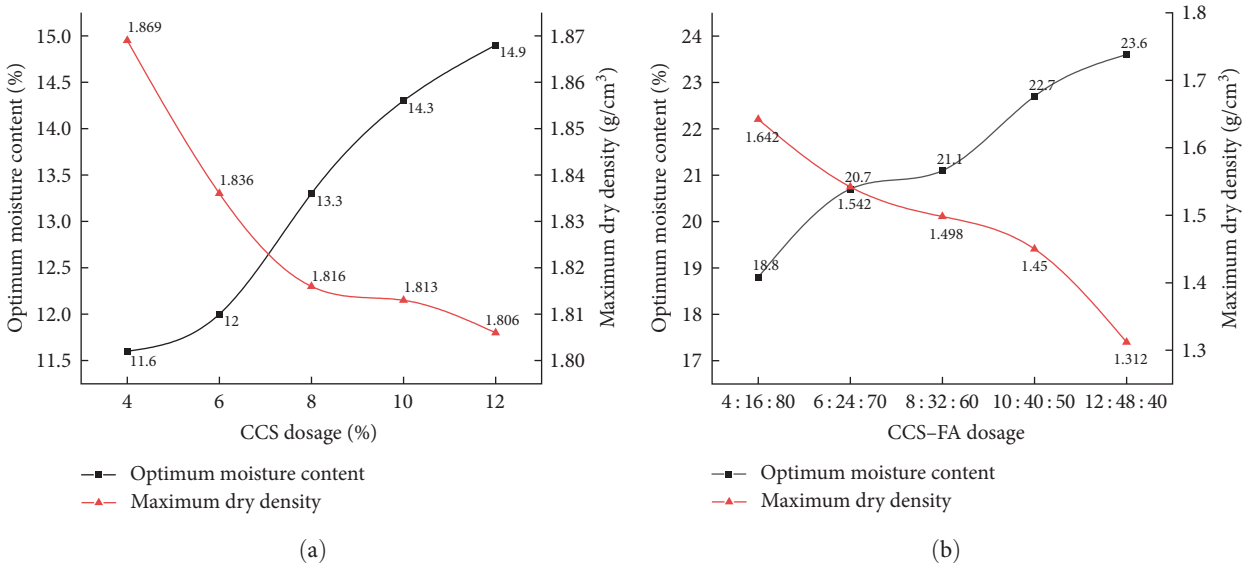

Figure 8: CCS-stabilized soil and CCS–FA-stabilized soil compaction test changes: (a) CCS-stabilized soil; (b) CCS–FA-stabilized soil.

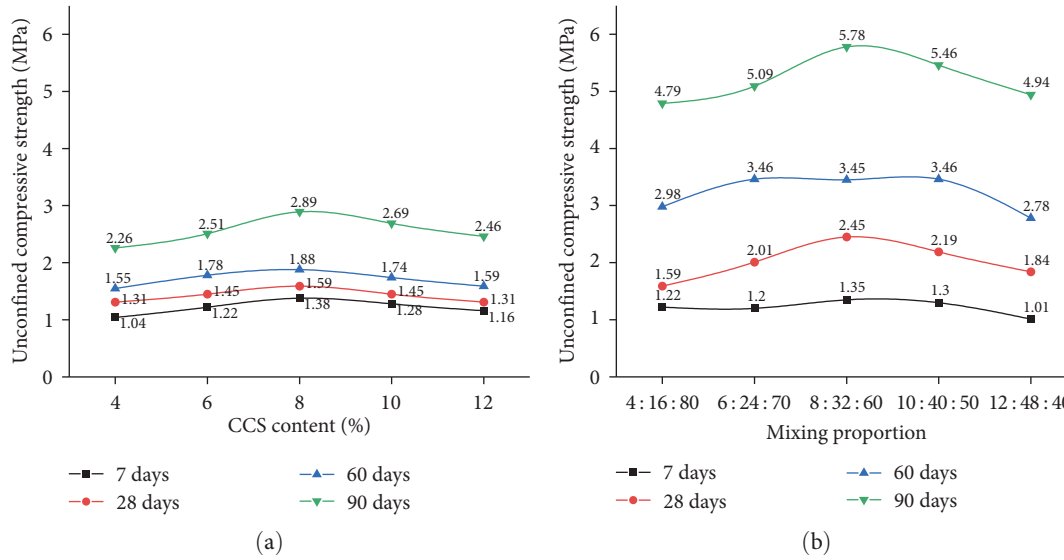

Figure 9: Unconfined compressive strength changes of CCS-stabilized soil and CCS–FA stabilized soil: (a) CCS-stabilized soil; (b) CCS–FA-stabilized soil.

As shown in Figure 9, the unconfined compressive strength of CCS-stabilized soil first increases and then decreases with increasing CCS content. When the CCS content is 8%, the unconfined compressive strength reaches a peak, and the strength at 7 and 90 days is 1.38 and 2.89 MPa, respectively. The unconfined compressive strength of CCS-stabilized soil at 8% CCS content is higher than that of 4% cement-stabilized soil, with early strength increasing faster than the later strength. The formation of strength in CCS-stabilized soil is primarily attributed to ion exchange and condensation phenomena. Upon hydrolysis and ionization, CCS ionizes Ca^{2+} and OH^{-}, leading to Ca^{2+} reacting with K^{+} and Na^{+} in the soil to form an adsorption system. The interaction between CCS and soil particles can alter the charged state of stabilized soil, leading to the reaggregation of soil particles and ions to form a more compacted ash soil particle cementation system, thereby enhancing the initial strength of CCS-stabilized soil. The results of the unconfined compressive strength test for CCS–FA-stabilized soil indicate that the unconfined compressive strength initially increases and then decreases with an increase in the proportion of the binder. The mixing proportion at the peak unconfined compressive strength at different ages is 8 : 32 : 60, with the unconfined compressive strength of CCS–FA-stabilized soil being 1.35 and 5.78 MPa, respectively, at 7 and 90 days. The addition of FA significantly increases the unconfined compressive strength of the stabilized soil, with the content of SiO_2 and Al_2O_3 in FA being higher. The pozzolanic reaction caused by the reaction is stronger than that of CCS-stabilized soil, thereby allowing the active potential of CCS to be fully realized. The C–S–H gel generated by the reaction effectively

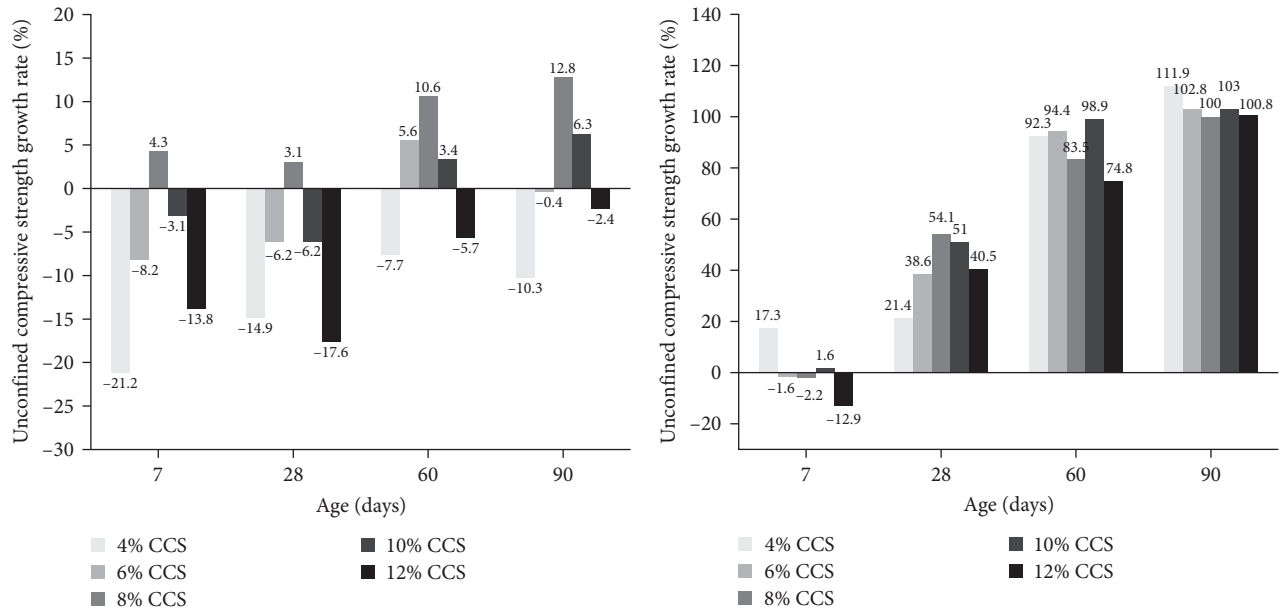

Figure 10: Comparison of CS, 4% cement soil, and FCS compressive strength: (a) CCS-stabilized soil; (b) CCS–FA-stabilized soil.

improves the internal void distribution of CCS–FA-stabilized soil, making the connection of soil particles more stable.

Based on Figure 10, it can be observed that for CCS-stabilized soil, there is a positive growth rate in unconfined compressive strength at different ages when the content of CCS is 8%. This suggests that the optimal effect is achieved when the CCS content is approximately 8%. Furthermore, a comparison of the unconfined compressive strength between CCS-stabilized soil and CCS-stabilized soil indicates that when the CCS content is identical, the 7 days unconfined compressive strength of the former increases at a faster rate than that of the latter.

4.3. Splitting Tensile Strength Test. The splitting strength test is conducted in accordance with the T0806-1994 method outlined in JTG E51-2009. The tensile strength of the split was evaluated using a universal material testing machine, an electric stripping machine, and a pavement strength testing machine. Initially, cylindrical samples with a diameter and height of 50 mm were prepared by compacting mixed materials of varying proportions via a static pressure technique using a universal material testing machine and based on the optimal water content and maximum dry density determined from the compaction test. The mixed materials were then sealed in plastic bags using an electric stripper. After the standard solidifies to the specified age, the sample is placed on the centerline of the arc surface pressing strip and kept perpendicular to the test plane to reduce testing errors. The width and radius of the arc surface pressing strip are 6.35 and 25 mm, respectively. Finally, a pavement strength testing machine was used to apply a loading rate of 1 mm/min, and the maximum pressure when the specimen was damaged was recorded to complete the splitting tensile strength test (see Figure 11). The test results are presented in Figure 12,

Figure 11: Splitting test.

and a comparison of the splitting strength between CCS-stabilized soil, 4% cement soil, and CCS–FA-stabilized soil is shown in Figure 13. In the reference group, the 7 28, 60, and 90 days splitting tensile strengths of 4% cement-stabilized soil were 0.12, 0.15, 0.21, and 0.31 MPa, respectively.

From Figure 12, it is evident that the splitting strength of the stabilized soil with CCS increases as the content of CCS increases. The early splitting strength increases rapidly, while the later splitting strength increases relatively slowly, which is similar to the formation mechanism of unconfined compressive strength. When the content of cement is 4% and CCS is 8%, the splitting strength shows little difference. Moreover, the cleavage strength of CCS–FA-stabilized soil gradually increases with the increase of binder. Figure 12

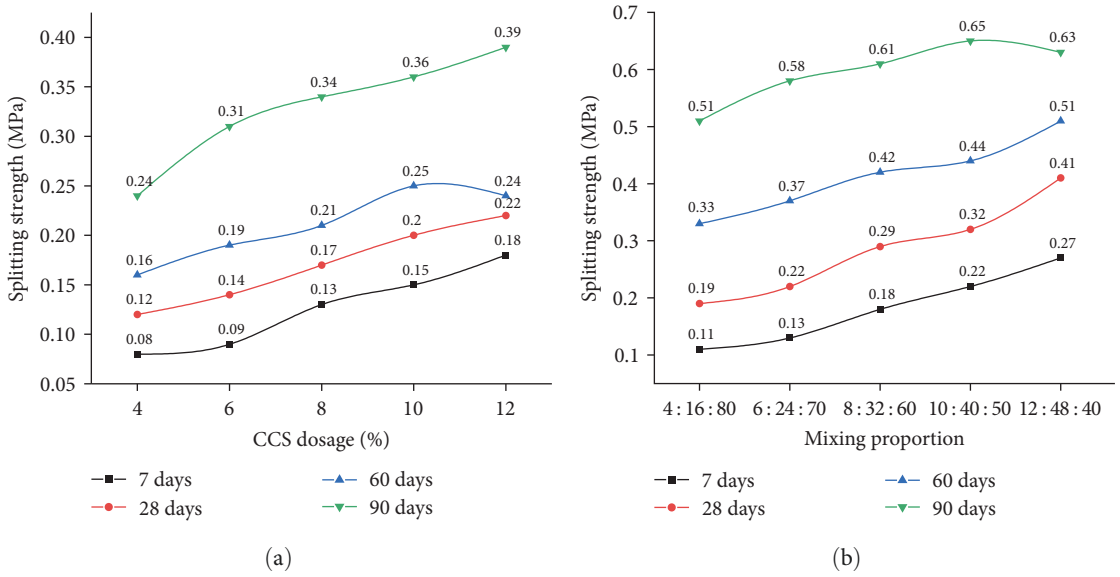

Figure 12: CCS-stabilized soil and CCS–FA-stabilized soil splitting strength changes: (a) CCS-stabilized soil; (b) CCS–FA-stabilized soil.

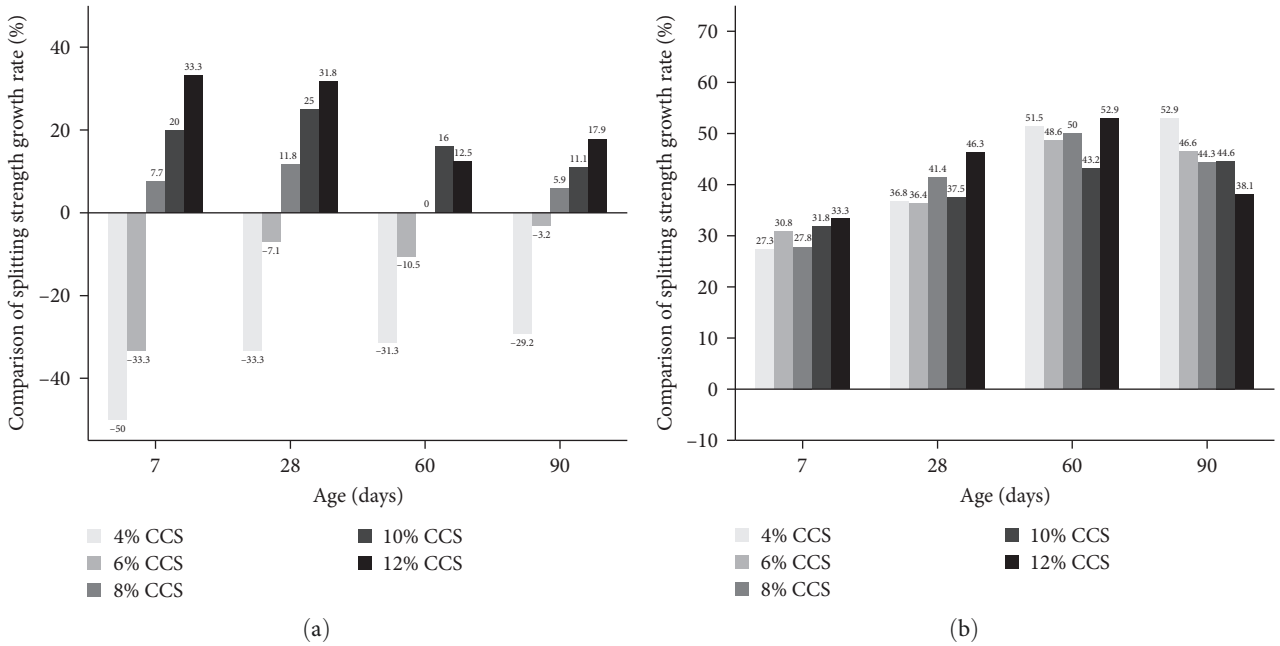

Figure 13: Comparison of splitting strength between CCS-stabilized soil and 4% cement soil and CCS–FA-stabilized soil: (a) CCS stabilized soil; (b) CCS–FA-stabilized soil.

shows that the cleavage strength at the age of 7 and 28 days increases faster than that at the age of 60 and 90 days, indicating a faster increase in the early strength of CCS–FA-stabilized soil. In the later stage of the reaction, volcanic ash reacts slowly to form C–S–H and C–A–H, which can improve the initial activation energy of the reaction [29, 30].

Through the evaluation of Figure 13, it can be observed that the early splitting electricity boom of CCS-stabilized soil is accelerated. However, CCS-stabilized soil containing 4% and 6% CCS content material, as well as 4% cement soil, exhibit poor growth, indicating that the former two have a detrimental impact and fail to meet the diagram requirements. Conversely, when the CCS content exceeds 8%, the splitting power experiences a positive growth rate in comparison to 4% cement soil, suggesting that the splitting power can meet the specifications when the CCS content exceeds 8%. Moreover, the impact of soil enchantment is remarkable; after comparing CCS-stabilized soil and CCS–FA-stabilized soil, it was found that the addition of FA can significantly improve the unconfined compressive strength and splitting strength of CCS-stabilized soil. As time passes, the splitting strength of the soil continues to increase. This can be attributed to the fact that the initial strength of CCS and soil results from ion exchange and condensation, while the later strength of CCS-stabilized soil is influenced by the volcanic ash reaction and carbonation reaction. However, the reaction

(a) (b)

Figure 14: Compressive elastic modulus test: (a) UTM universal material testing machine; (b) compressive elastic modulus test.

process is slow, and the increase in depth is relatively slow as well, particularly in the later stages. The enhancement and lasting impact of volcanic ash response have an influence on the depth [31].

4.4. Compressive Modulus of Resilience Test. The compressive modulus of resilience is employed to characterize the recoverable deformation characteristics of the subgrade under immediate loading. A higher modulus of resilience indicates a greater capacity of the soil foundation to withstand external loads. The compressive resilience modulus test is conducted in accordance with the T0808-1994 method in JTG E51-2009. The top surface method is employed to test the compressive resilience modulus, mainly utilizing equipment such as the universal material testing machine, electric stripping machine, pavement strength testing machine, and universal material testing machine (UTM). First, cylindrical samples with a diameter of 100 mm and height of 100 mm were prepared through the universal material testing machine by the static pressure of mixed materials with different proportions based on the optimal water content and maximum dry density determined by the compaction test. The mixed materials were subsequently sealed with plastic bags using an electric stripper. After curing for 180 days using standard curing methods, a UTM was used to conduct tests, as shown in Figure 14. The two end faces of the cylindrical specimens were thoroughly smoothed with cement slurry. The specimens were saturated with water for 24 hr, with the water level approximately 2.5 cm above the top surface of the specimen. A unit pressure of 0.4 MPa was selected on the loading plate, and the calculation program was set on the UTM universal material testing machine. After the specimens were wiped dry with a cloth following the 24 hr saturation, they were placed on the loading baseplate. A small amount of fine sand (0.25–0.5 mm) was sprinkled on the top surface of the specimen to fill in any microscopic irregularities and increase the contact area between the top platen and the specimen surface. Two preloading–unloading tests were performed with half of the maximum load applied to ensure tight contact between the loading top platen and the specimen surface. Each unloading took 1 min. The unit pressure was then divided into five equal parts as the pressure value for each application. The first level of load was applied, and after 1 min, the readings during loading were recorded. The load was then removed, allowing the elastic deformation of the specimen to recover. The readings during unloading were recorded at 0.5 min. The difference between the loading and unloading readings was calculated as the rebound deformation under this load level. This process was repeated for each level of loading and unloading until the rebound deformation under the last level was recorded. Finally, a relationship curve was plotted with unit pressure as the abscissa and rebound deformation as the ordinate. The first and second test points were connected by a straight line, extended to intersect the coordinate axis, and the data were corrected and fitted to obtain the compressive resilience modulus. The results of the test are presented in Figure 15, and the compressive modulus of resilience of 4% cement-stabilized soil, CCS-stabilized soil, and CCS–FA-stabilized soil are compared in Figure 16. The 7, 28, 60, and 90 days modulus of compressive resiliences of 4% cement-stabilized soil in the reference group were 258, 386, 452, and 591 Mpa, respectively.

Figure 15 shows that the compressive modulus of resilience of CCS-stabilized soil initially increases and then decreases with increasing CCS content. The compressive modulus of resilience of 8% CCS-stabilized soil is comparable to that of 4% cement-stabilized soil but greater than that of 4% cement-stabilized soil. Similarly, the compressive modulus of resilience of CCS–FA-stabilized soil initially increases and then decreases. The maximum compressive modulus of resilience at 90 days is 1,124 MPa, achieved with a mixing ratio of 8 : 32 : 60. Compared to stabilized soil with CCS alone, the addition of FA leads to a significant improvement in compressive modulus of resilience, resulting in higher strength, less deformation, and greater bearing capacity. This indicates that CCS–FA-stabilized soil exhibits greater resistance to deformation [25].

From Figure 16, it can be observed that the impact of improving the compressive modulus of resilience is no longer significant when comparing 4% cement-stabilized soil and CCS-stabilized soil. For CCS-stabilized soil with a content of 8%, there is a positive increase in compressive modulus of resilience for 7, 60, and 90 days, with an increased rate of 8.4% for 28 days. However, when compared to 4%, CCS-stabilized soil with other contents showed negative growth rates for 7 and 28 days. With the extension of the curing age,

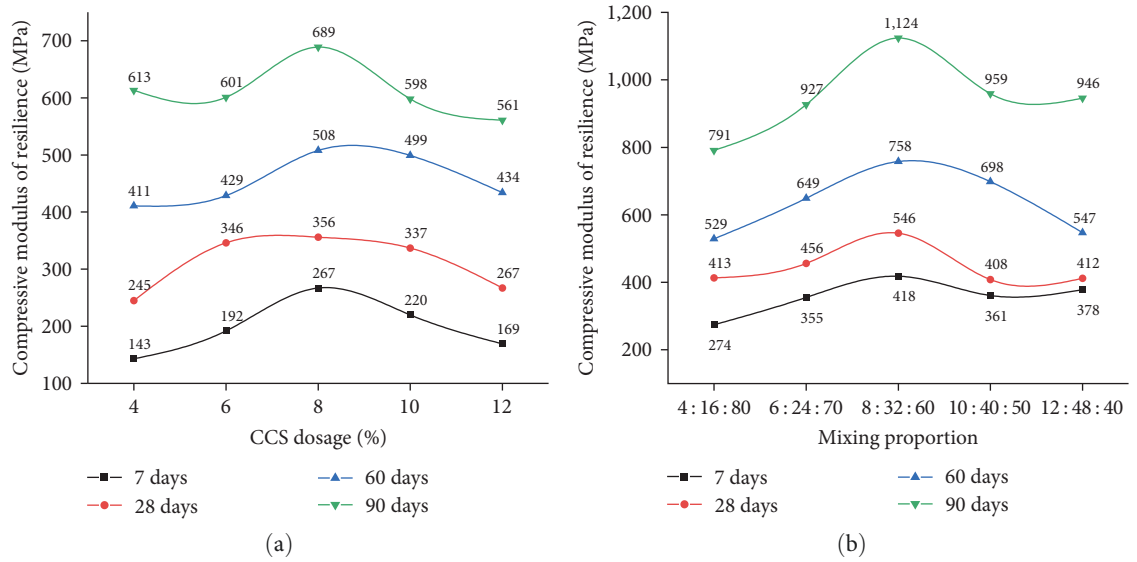

Figure 15: Compressive modulus of resilience of CCS-stabilized soil and CCS–FA-stabilized soil: (a) CCS-stabilized soil; (b) CCS–FA-stabilized soil.

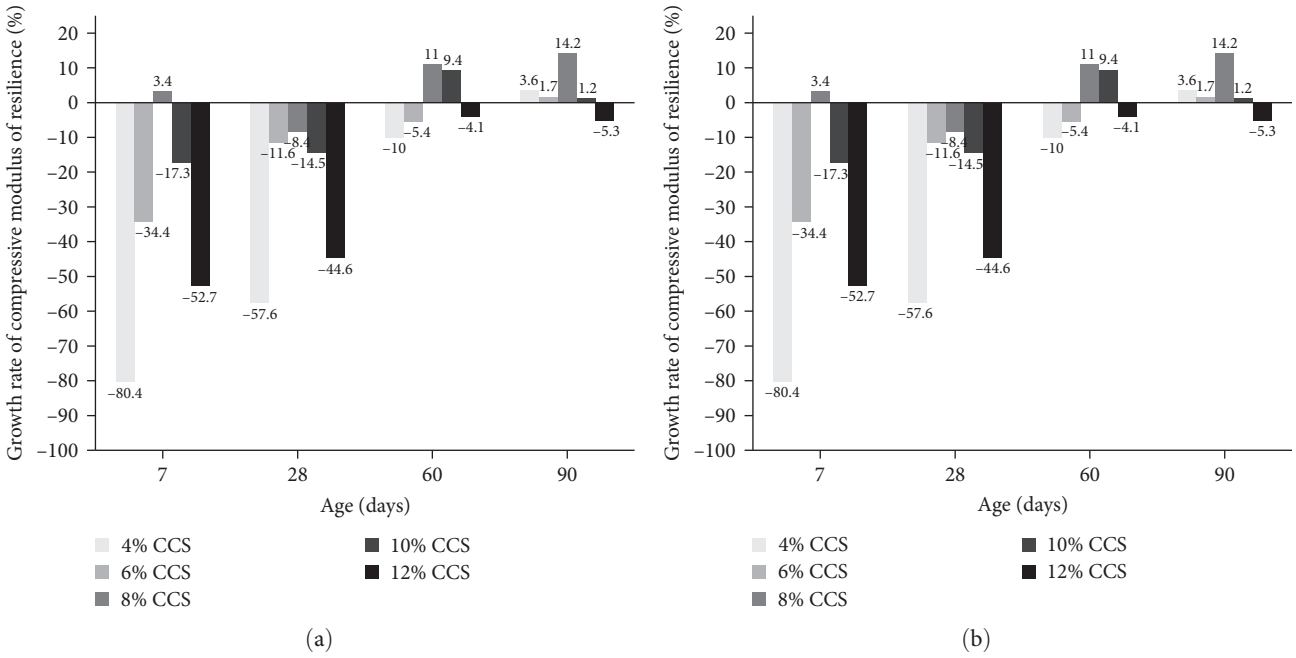

Figure 16: Comparison of compressive modulus of resilience of 4% cement-stabilized soil, CCS-stabilized soil, and CCS–FA-stabilized soil: (a) CCS-stabilized soil; (b) CCS–FA-stabilized soil.

the compressive modulus of resilience of CCS-stabilized soil progressively increases, surpassing that of 4% cement-stabilized soil. This suggests that CCS-stabilized soil initially exhibits poor deformation resistance, but over time, its modulus of resilience gradually increases, and its deformation resistance improves accordingly. Notably, the stabilized soil with 8% CCS shows the best performance. Comparing CCS-stabilized soil with CCS–FA-stabilized soil, the compressive resilient modulus of CCS–FA-stabilized soil is higher, indicating a significant improvement in its ability to resist deformation. Moreover, the 7 day compressive modulus of resilience of CCS–FA-stabilized soil exhibits the fastest growth rate, far surpassing that of CCS-stabilized soil. These findings indicate that the addition of FA can substantially enhance the resilient modulus of stabilized soil and its ability to resist deformation [32–34].

4.5. California Bearing Ratio Test. The bearing capacity of a soil foundation increases with a higher California bearing ratio (CBR) value. The CBR test is conducted following the T0134-2019 method in JTG 3430-2020. The test is typically performed using a multifunctional automatic electric compacting instrument or a

Figure 17: California bearing ratio test.

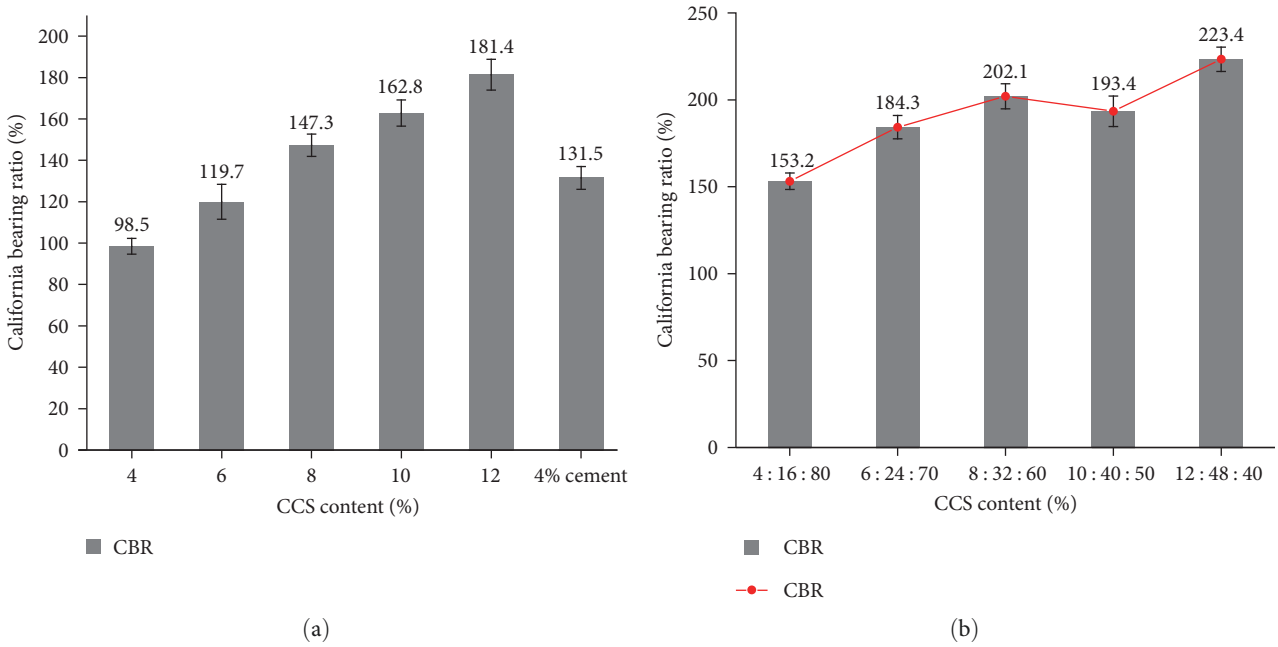

Figure 18: Change trend of CS and FCS load-bearing ratio: (a) CCS-stabilized soil; (b) CCS–FA-stabilized soil.

pavement strength testing machine. The mixed materials of varying proportions are compacted using the instrument to form cylindrical specimens with a diameter and height of 150 mm based on the optimum water content and maximum dry density determined through compaction testing. The specimens are then immersed in water for 4 days and subjected to a penetration test using a pavement material tester (refer to Figure 17). The penetration rod is pressed into the specimen at a rate of 1 mm/min, and five or more readings are taken when the penetration amount reaches 2.5 mm. A relationship curve is then drawn between the penetration amount and unit pressure, and the bearing ratio is calculated at a penetration volume of 2.5 mm. The CBR value for the reference group of 4% cement-stabilized soil was 131.5%. The check effects and a comparison of CCS-stabilized soil, CCS–FA-stabilized soil, and 4% cement-stabilized soil CBR can be seen in Figures 18 and 19, respectively.

According to the test results presented in Figure 18, the CBR of CCS-stabilized soil increases steadily with an increase in CCS content. Notably, the CBR of 4% cement-stabilized soil reaches 131.5%, which falls within the range of 6%–8% of the bearing ratio strength of CCS-stabilized soil. This finding suggests that the bearing ratio at 8% of CCS content is sufficient to meet the subgrade bearing capacity requirements and meet the minimum specification requirements. Additionally, the CBR of CCS–FA-stabilized soil gradually increases. The

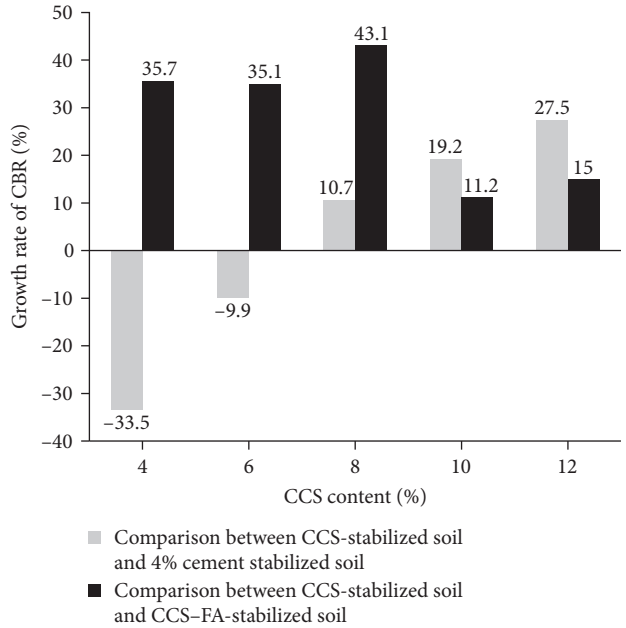

Figure 19: Comparison of CCS-stabilized soil, CCS–FA-stabilized soil, and 4% cement-stabilized soil CBR.

maximum CBR of 259.1 MPa differs by only 2.24% from the minimum CBR, thereby satisfying the minimum CBR requirements for subgrade filling in the specification [35].

In Figure 19, the contrast shows that there is a positive increase in the CBR of CCS-stabilized soil when the CCS content material increases from 4% to 8%, in comparison to cement-stabilized soil. This suggests that the CBR of CCS-stabilized soil with 8% content material can reach that of cement-stabilized soil with 4% content. Additionally, for CCS–FA-stabilized soil, the CBR shows a positive growth rate, indicating that the addition of FA can significantly improve the bearing capacity of stabilized soil and enhance the balance of subgrade strength [36, 37].

5. Conclusions

The overall performance of CCS-stabilized soil and CCS–FA-stabilized soil under different content was analyzed through laboratory testing. The following are the key findings:

(1) The results of the unconfined compressive strength test indicate that the maximum compressive strength for the 7 and 28 day CCS and FA binders are 1.24 and 5.61 MPa, respectively. Therefore, the optimal mixing ratio of CCS and FA binder is determined to be 20 : 80 (1 : 4). Based on the unconfined compressive strength test results of CCS-stabilized soil, the mixing ratio of CCS–FA-stabilized soil under maximum stress is determined to be 8 : 32 : 60. The FA content has high amounts of SiO_2 and Al_2O_3. The pozzolanic reaction effectively forms C–S–H gel, which improves the internal void distribution of CCS–FA-stabilized soil, thereby enhancing the stability of soil particle connection.

(2) With the expansion of the content of CCS, both the splitting strength and CBR increase. When the content of CCS ranges from 6% to 8%, the splitting strength of stabilized soil with CCS can reach up to 4% of that of the cement-stabilized soil. Moreover, when the proportion of CCS–FA-stabilized soil is 8 : 32 : 60, the splitting power can also reach 4% of the cement-stabilized soil. Additionally, the early energy of CCS–FA-stabilized soil will increase rapidly, and volcanic ash reacts slowly to shape C–S–H and C–A–H, indicating that FA can enhance the preliminary activation strength of the reaction.

(3) With the amplify of the content material of CCS–FA, the resilient modulus of CCS-stabilized soil and CCS–FA-stabilized soil tends to make bigger first and then decrease. The highest quality mixing ratio of CCS-stabilized soil is 8 : 92 and that of CCS–FA-stabilized soil is 8 : 32 : 60. The addition of FA can drastically beautify the resilient modulus of stabilized soil and its capability to withstand deformation.

In conclusion, it is endorsed that the excellent percentage of CCS and FA binder is 1 : 4, the satisfactory share of CCS-stabilized soil is 8 : 92, and the nice share of CCS–FA-stabilized soil is 8 : 32 : 60.

Data Availability

The data used to support the findings of this study are included within the article.

Conflicts of Interest

The authors declare that they have no conflicts of interest.

Authors' Contributions

Yanxia Cai made the research plan and checked the article content; Zhishu Zang analyzed the test results and wrote the article; Xiaolin Zuo investigated the relevant research results obtained in the article; Fengtao Liu carried out experimental research and collated test results; Lengxue Li carried out experimental research and collated test results; Kaiji Lu made the research plan and checked the article content; Qianlong Huang carried out experimental research and wrote the article.

References

[1] Ministry of Transport, "Statistical bulletin of transport industry development in 2022," *China Communications News*, 2023-06-16(002), 2023.

[2] Engineering Risk and Insurance Research Branch of China Civil Engineering Society, "Anhui section of Yuexi Wuhan expressway," *Urban and Rural Development*, vol. 17, pp. 78-79, 2021.

[3] W. Jie, "Discussion on road construction materials in civil engineering," *Residential Industry*, vol. 2, pp. 17–19, 2020.

[4] T. K. Rajak, L. Yadu, and S. K. Pal, "Analysis of slope stability of fly ash stabilized soil slope," in *Geotechnical Applications*, I. V. Anirudhan and V. B. Maji, Eds., vol. 13 of *Lecture Notes in Civil Engineering*, pp. 119–126, Springer, Singapore, 2019.

[5] A. Arulrajah, A. Mohammadinia, I. Phummiphan, S. Horpibulsuk, and W. Samingthong, "Stabilization of recycled demolition aggregates by geopolymers comprising calcium carbide residue, fly ash and slag precursors," *Construction and Building Materials*, vol. 114, pp. 864–873, 2016.

[6] W. Li and Y. Yi, "Use of carbide slag from acetylene industry for activation of ground granulated blast-furnace slag," *Construction and Building Materials*, vol. 238, Article ID 117713, 2020.

[7] X. Gong, T. Zhang, J. Zhang et al., "Recycling and utilization of calcium carbide slag-current status and new opportunities," *Renewable and Sustainable Energy Reviews*, vol. 159, Article ID 112133, 2022.

[8] F. Darikandeh, "Expansive soil stabilised by calcium carbide residue-fly ash columns," *Proceedings of the Institution of Civil Engineers-Ground Improvement*, vol. 171, no. 1, pp. 49–58, 2018.

[9] Y. Xiuming, Y. Xiaohua, and W. Hongbing, "Study on the application of fly ash and carbide slag mixture as subgrade filler," *Highway Traffic Science and Technology (Application Technology Edition)*, vol. 5, pp. 91–93, 2007.

[10] G. Peng, D. Zengqi, L. Peilong, S. Minghan, and Z. Xianjun, "Analysis of factors affecting the strength of carbide slag fly ash stabilized soil," *Subgrade Works*, vol. 5, pp. 6–10, 2020.

[11] D. D. B. Nergis, P. Vizureanu, and O. Corbu, "Synthesis and characteristics of local fly ash based geopolymers mixed with natural aggregates," *Revista de Chimie*, vol. 70, no. 4, pp. 1262–1267, 2019.

[12] A. A. H. Sinan, C. Gülser, and M. Azab, "Potential of using fly ash as amendment for soil characteristics," 2022.

[13] T. P. Mashifana, F. N. Okonta, and F. Ntuli, "Geotechnical properties and microstructure of lime-fly ash-phosphogypsum-stabilized soil," *Advances in Civil Engineering*, vol. 2018, Article ID 3640868, 9 pages, 2018.

[14] B. D. Nath, M. K. A. Molla, and G. Sarkar, "Study on strength behavior of organic soil stabilized with fly ash," *International Scholarly Research Notices*, vol. 2017, Article ID 5786541, 6 pages, 2017.

[15] X. Qin, Y. Du, S. Liu, M. Wei, and Y. Zhang, "Experimental study on physical mechanics of calcium carbide slag modified over wet clay," *Journal of Geotechnical Engineering*, vol. 35, no. S1, pp. 175–180, 2013.

[16] P. Li, C. Zhao, Y. Pei, and J. Hu, "Study on composition design and influencing factors of carbide slag stabilized soil," *Highway Engineering*, vol. 46, no. 3, pp. 129–255, 2021.

[17] H. Y. Leong, D. E. L. Ong, J. G. Sanjayan, A. Nazari, and S. M. Kueh, "Effects of significant variables on compressive strength of soil-fly ash geopolymer: variable analytical approach based on neural networks and genetic programming," *Journal of Materials in Civil Engineering*, vol. 30, no. 7, Article ID 04018129, 2018.

[18] J. Liu, J.-H. Doh, H. L. Dinh, D. E. L. Ong, G. Zi, and I. You, "Effect of Si/Al molar ratio on the strength behavior of geopolymer derived from various industrial waste: a current state of the art review," *Construction and Building Materials*, vol. 329, Article ID 127134, 2022.

[19] P. Wei, Y. Chaoliang, Y. Guangqing, and D. Junxia, "Feasibility study on improving saline soil subgrade in coastal area with calcium carbide," *Geotechnical Mechanics*, vol. 30, no. 4, pp. 1068–1072, 2009.

[20] X. Longshan, *Study on the Influence of Calcium Carbide Slag on the Stability of Expansive Soil*, Guangxi University, 2012.

[21] N. Latifi, F. Vahedifard, E. Ghazanfari, and A. S. A. Rashid, "Sustainable usage of calcium carbide residue for stabilization of clays," *Journal of Materials in Civil Engineering*, vol. 30, no. 6, Article ID 04018099, 2018.

[22] L. Jie, *Study on Multi-Level Application for Three Types Industrial Waste Residue on First Class Highway*, Wuhan Polytechnic University, 2012.

[23] D. Honghui, *Application of Lime Improved Expansive Soil in Expressway Subgrade Filling*, Southeast University, 2006.

[24] L. Yuyi, L. Xiongwei, S. Yuexin, W. Hui, D. Wenchuang, and L. Shunkang, *Research progress of carbide slag pozzolanic composite solidified soil. Environmental Engineering 2018 National Academic Annual Meeting*, pp. 252–258, 2018.

[25] R. Kou, M.-Z. Guo, L. Han et al., "Recycling sediment, calcium carbide slag and ground granulated blast-furnace slag into novel and sustainable cementitious binder for production of eco-friendly mortar," *Construction and Building Materials*, vol. 305, Article ID 124772, 2021.

[26] Y. Liu, C.-W. Chang, A. Namdar et al., "Stabilization of expansive soil using cementing material from rice husk ash and calcium carbide residue," *Construction and Building Materials*, vol. 221, pp. 1–11, 2019.

[27] F. Akcanca and M. Aytekin, "Effect of wetting—drying cycles on swelling behavior of lime stabilized sand-bentonite mixtures," *Environmental Earth Sciences*, vol. 66, pp. 67–74, 2012.

[28] W. Jianwei, "Study on mechanical properties of cement red mud fly ash stabilized soil stabilizer," *Tianjin Construction Science and Technology*, vol. 32, no. 1, pp. 56–60, 2022.

[29] N.-J. Jiang, Y.-J. Du, S.-Y. Liu, M.-L. Wei, S. Horpibulsuk, and A. Arulrajah, "Multi-scale laboratory evaluation of the physical, mechanical, and microstructural properties of soft highway subgrade soil stabilized with calcium carbide residue," *Canadian Geotechnical Journal*, vol. 53, no. 3, pp. 373–383, 2015.

[30] Z. Hongzhou, T. Limei, W. Shuang, and Q. Yanghong, "Experimental study on engineering properties of fiber-stabilized carbide-slag-solidified soil," *PLoS ONE*, vol. 17, no. 4, Article ID e0266732, 2022.

[31] L. Peilong, B. Jiayu, P. Yi, and Z. Dejian, "Performance improvement analysis of fly ash on calcium carbide slag stabilized loess," *Highway Engineering*, vol. 47, no. 6, pp. 146–152, 2022.

[32] Z. Kaijian, *Research and Application of Key Technologies of Industrial Solid Waste in Subgrade Engineering*, Hebei University of Engineering, 2021.

[33] L. Fengtao and H. Qianlong, "Experimental study on mechanical properties of subgrade treated with carbide slag stabilized soil," *China Highway*, vol. 10, pp. 108-109, 2022.

[34] Z. Lu, "Study on the detection method of cement lime dosage of cement stabilized soil," *Fujian Construction Science and Technology*, vol. 5, pp. 52-53, 2021.

[35] Y. Banglin, "Test analysis of carbide slag fly ash stabilized soil subbase," *Science and Technology Information*, vol. 24, pp. 359-360, 2013.

[36] Y. Bo, L. Xin, C. Fuke, and Z. Huixian, "Research on the application of industrial waste residue composite material to stabilize expansive soil," *Subgrade Works*, vol. 4, pp. 77–81, 2020.

[37] L. Yong, "Experimental study on the strength of cement stabilized soil with natural mineral soil stabilizer," *Hunan Transportation Science and Technology*, vol. 43, no. 3, pp. 75–97, 2017.